ISSN 0016-7932, Geomagnetism and Aeronomy, 2015, Vol. 55, No. 5, pp. 585–595. © Pleiades Publishing, Ltd., 2015.
Original Russian Text © V.G. Vorobjev, O.I. Yagodkina, E.E. Antonova, 2015, published in Geomagnetizm i Aeronomiya, 2015, Vol. 55, No. 5, pp. 611–622.

Features of the Planetary Distribution of Ion Precipitation at Different Levels of Magnetic Activity

V. G. Vorobjev[a], O. I. Yagodkina[a], and E. E. Antonova[b, c]

[a] *Polar Geophysical Institute, Apatity, Murmansk Oblast, Russia*
[b] *Skobeltsin Nuclear Physics Research Institute, Moscow State University, Moscow, Russia*
[c] *Space Research Institute, Moscow, Russia*
e-mail: vorobjev@pgia.ru

Received April 20, 2015

Abstract—Observations from DMSP *F*6 and *F*7 spacecraft were used to examine the features of the planetary distribution of ion precipitation. Ion characteristics were defined within the boundaries of different types of auroral electron precipitation, which in accordance with the conclusions from (Starkov et al., 2002) were divided into a structured precipitation of an auroral oval (AOP) and zones of diffuse precipitation DAZ and SDP located equatorward and poleward of AOP, respectively. Analogous to electron precipitation, ion precipitation did not demonstrate dependences of the average energy and the average energy flux of precipitating particles on the *Dst* index value. In the diffuse precipitation zone (DAZ) equatorward of the auroral oval, ion energies clearly peaked in the sector of 1500–1800 MLT. The average energy value grows as magnetic activity increases from ~12 keV at $AL = -1000$ nT to ~18 keV at $AL = -1000$ nT. In the region of structured precipitation (AOP), the minimum of the average ion energy is observed in the dawn sector of 0600–0900 MLT. Ion energy fluxes (F_i) are maximal in the nighttime MLT sectors. In the zone of soft diffuse precipitation (SDP) poleward of AOP, the highest ion energy fluxes are observed in the daytime sector, while the nightside F_i values are insignificant. Ion energy fluxes in the SDP zone show an anticorrelation with the average ion energy in the same MLT sector. An ion precipitation model was created which yields a global distribution of both the average ion energies and the ion energy fluxes depending on the magnetic activity expressed by *AL* and *Dst* indices. Comparison of this model with the model of electron precipitation shows that the planetary power of ion precipitation at low magnetic activity ($|AL| = 100$ nT) is ~12% of the electron precipitation power and exponentially decreases to ~4% at $|AL| > 1000$ nT. The ion precipitation model was used to calculate the plasma pressure at the ionospheric altitudes. The planetary distribution of integral ionospheric conductance depending on the magnetic activity was calculated by using both electron and ion precipitation models.

DOI: 10.1134/S0016793215050187

INTRODUCTION

Along with electron precipitation, auroral ion precipitation plays a noticeable role in physical-chemical processes of the high-latitude ionosphere. The fluxes of precipitating ions (predominantly protons) create additional ionization, which can considerably contribute to ionospheric conductance (Galand and Richmond, 2001; Galand et al., 2001). The same fluxes determine plasma pressure at the ionosphere altitudes (Wing et al., 1998; Stepanova et al., 2002, 2006), make a certain contribution to the luminosity of main auroral emissions, and excite the luminosity of specific hydrogen emissions in precipitation zones (Coumans et al., 2002). Research on ion precipitation characteristics is carried out by both ground-based and satellite methods. Optical observations by high-apogee satellites allow the researchers to obtain a nearly "instant" distribution of the luminosity of different emissions on a planetary scale. However, recalculation of the luminosity intensities of different emissions into either electron or ion precipitation characteristics implies the application of different assumptions and a set of coefficients that are not always reliably known. The solution of such an inverse task is therefore connected with large errors that often have undeterminable values.

Direct satellite observations provide "instant" precipitation characteristics along the flight path. Additionally, the application of a great amount of statistical data enables the construction of a planetary precipitation distribution model. Such a model shows the mean characteristics of different precipitation types, and these characteristics can considerably differ from the "instant" precipitation pattern. To construct statistically average planetary precipitation models, DMSP satellite observations are often used, because these satellites operate on circular polar orbits at a height of ~835 km for more than two decades. The orbits of these satellites are conditionally oriented in the dawn–dusk and midday–midnight directions. Since the orbits are stabilized relative to the Earth's rotation axis, the diurnal precession of the geomagnetic pole relative to the geographic one leads to the fact that the

orbits cover nearly all longitudes of local geomagnetic time, especially one considers orbits in both hemispheres. SSJ/4 electrostatic analyzers on board the DMSP satellites record the fluxes of precipitating electrons and ions in the energy band from 32 eV to ~30 keV in 19 energy channels for each population.

The statistically founded model of ion precipitation was proposed for the first time in (Hardy et al., 1989). This model, which was based on data from the DMSP *F*6 and *F*7 satellites, utilized a 3-h *Kp* index as the geomagnetic activity parameter. Since the *Kp* index does not, however, characterize the level of magnetic activity during the satellite passage (about 3–5 min) through the precipitation zone, the model from (Hardy et al., 1989), while advanced in its time, provides a quite rough estimate of average energies and energy fluxes of precipitating particles. More advanced models were presented in (Newell et al., 2004, 2009). In (Newell et al., 2004), maps of planetary precipitation distribution were presented for all quadrants of *Bz* and *By* orientations of the interplanetary magnetic field (IMF); in (Newell et al., 2009), a precipitation model was constructed with respect to the solar wind parameters. These models are very useful for research purposes owing to the large database and high resolution in terms of the MLat–MLT (geomagnetic latitude–local magnetic time) coordinate system. However, due to the specificity of their input parameters, they are hardly applicable for both the study of precipitation characteristics in periods of geomagnetic disturbances and their comparison with the planetary distributions of such geophysical phenomena as auroral luminosity, auroral and geomagnetic pulsations, ionospheric currents, riometric absorption, and others.

In (Vorobjev et al., 2013a), the auroral precipitation model (APM) was presented; this model shows the planetary distribution of different electron precipitation zones and the characteristics of precipitating electrons with respect to the magnetic activity level expressed by *AL* and *Dst* indices. The model is available on the Internet (http://apm.pgia.ru). In (Vorobjev et al., 2013a), the APM was used to investigate the behavior of different ionospheric and magnetospheric parameters during disturbances, while in (Vorobjev et al., 2013b) it was applied to calculate the global distribution of auroral luminosity in different spectral regions.

In order to obtain a more complete pattern of precipitations, the APM should be supplemented with ion precipitation characteristics. Vorobjev and Yagodkina (2014) studied the comparative characteristics of the electron and ion precipitation in the dawn and dusk sectors based on the data from the DMSP *F*6 and *F*7 satellites. It was shown that the boundaries of electron and ion precipitation in the dusk sector nearly coincide at all magnetic activity levels. In the dawn sector, however, the electron precipitation zone was 3°–4° wider than the ion precipitation zone. The ion energy fluxes in the equatorial part of precipitation zones were insignificant here and was as low as 0.02–0.05 erg/cm^2 at all magnetic activity levels.

The goal of this article is to investigate the ion precipitation characteristics in all MLT sectors; to obtain the global ion precipitation pattern with respect to the magnetic activity level; and to apply the precipitation models in the calculation of plasma pressure at the ionosphere altitudes and in the construction of a planetary model of integrated ionospheric conductance.

2. DATA

To investigate the ion precipitation characteristics, we chose the same passes of the DMSP *F*6 and *F*7 satellites as those used for the APM construction. The database contains more than 32 000 crossings of auroral precipitation zones by satellites in both hemispheres during 1986. Although this year was remarkable for its minimum in terms of solar activity, significant magnetospheric disturbances were observed, including a great magnetic storm in February, with a maximum *Dst* = –307 nT (http://wdc.kugi.kyoto-u.ac.jp/dst_final/198602/index.html). In addition to the characteristics of ion and electron precipitations, the database contains such parameters as (a) *Dst* index, (b) 5-min *AL* index values, (c) hourly IMF values, (d) hourly values of solar wind parameters, and (e) phases of substorm for each satellite transit through the auroral zone.

In the frame of present investigation the characteristics of precipitating ion were examined within the boundaries of different type auroral precipitations which earlier (Starkov et al., 2002) were divided into three precipitation zones:

—*DAZ* (diffuse auroral zone) is the region of diffuse precipitation which located equatorward of auroral oval spatially coincides with the diffuse auroral zone;

—*AOP* (auroral oval precipitation) is the region of structured auroral precipitation with the poleward and equatorward boundaries statistically coinciding with the boundaries of auroral oval;

—*SDP* (soft diffuse precipitation) is the region of diffuse precipitation poleward of AOP.

To increase the statistical significance of the results, all of the data were grouped into eight 3-h intervals on MLT (0000–0300 MLT, 0300–0600 MLT, and so on). For each of these intervals, the mean characteristics of precipitating particles were determined with respect to the magnetic activity level. A detailed description of the database structure, as well as the nomenclature and positions of precipitation boundaries, are discussed in (Vorobjev et al., 2013a) and in references therein.

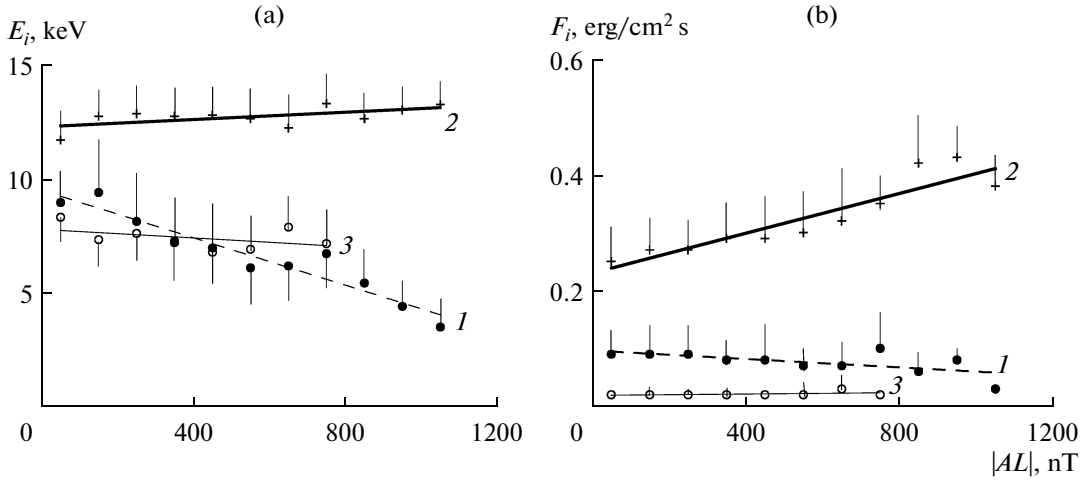

Fig. 1. Average ion energies (a) and ion energy fluxes (b) in the sector 2100–2400 MLT depending on the value of 5-min *AL* index in different precipitation zones: DAZ, dashed solid lines *1* and filled circles; AOP, thick lines *2* and crosses; SDP, thin solid lines *3* and empty circles.

3. PLANETARY CHARACTERISTICS OF ION PRECIPITATIONS

To construct the ion precipitation model in each 3-h MLT interval, we studied the average energies (E_i) and energy fluxes (F_i) of precipitating ions in the DAZ, AOP, and SDP zones with respect to the magnetic activity level. Regression equations were then defined to link E_i and F_i with magnetic activity, and the planetary model was constructed on the basis of the boundary positions of different precipitation types from the APM and with respect to the values of *AL* and *Dst* indices. As an example, the influence of magnetic activity on precipitating ion characteristics in the sector 2100–2400 MLT is shown in Fig. 1. The choice of this longitudinal interval is based on the fact that the main processes related to substorm development run here. In (Liou et al., 2001), 648 cases of auroral breakups (substorm onsets) observed in the UV spectral region from Polar satellite were investigated. It was shown that 85% of auroral breakups were recorded in the sector 2100–2400 MLT.

It should be noted that no dependence has been found between the average energies and energy fluxes of precipitating particles, on the one hand, and *Dst* index values, on the other hand, for either ion and electron precipitation. In other words, in all precipitation zones and in all MLT sectors, the characteristics of precipitating particles do not depend on magnetic storm intensities. The *Dst* index value is determined by the DR current intensity and the intensity of currents across the magnetosphere tail (Maltsev, 2004). These currents considerably affect the positions of different precipitation boundaries, the areas of precipitation, and hence the total precipitation power, but not the characteristics of precipitating particles.

Figure 1 shows average energies (a) and energy fluxes (b) of ions in the DAZ, AOP, and SDP precipitation zones in the sector 2100–2400 MLT, depending on the value of the 5-min *AL* index. Mean values of E_i and F_i were determined in the intervals of $|AL|$ with 100-nT step (0–100, 100–200 nT, and so on). For simplicity, the vertical lines on both sides denote half mean square deviations. The data were approximated by a linear polynomial. Line *1* (dashed line and filled circules) corresponds to the DAZ zone; line *2* (thick solid line and crosses) corresponds to the AOP zone; line *3* (thin solid line and empty circles) corresponds to the SDP zone. Since the SDP zone width rapidly reduces in the midnight sectors with growth of magnetic activity and this zone almost (and in fact) disappears at $|AL| > 600$ nT (Vorob'ev et al., 2000; Vorobjev et al., 2013a), the data on this zone in all figures are limited at $|AL| < 800$ nT.

Figure 1a shows that the avergae energies of precipitating ions in the AOP (2) and SDP (3) zones do not depend, in fact, on the *AL* index. This result most probably indicates that ion acceleration and deceleration in the zone of auroral "bulge" either do not play a significant role or compensate each other. However, energy flux of precipitating ions in the AOP zone increases with an increase in magnetic activity; at constant energy, this corresponds to an increase in ion concentration. The small increase in F_i with increasing $|AL|$ value is observed in the SDP zone.

In the diffuse zone located equatorward of the auroral oval (line *1*), considerable softening in spectrum of precipitating ions is observed with increased magnetic activity (Fig. 1a). Average ion energies decrease from 8-10 keV under quiet conditions to 3–5 keV at $|AL| \sim 1000$ nT. Ion energy flux (Fig. 1b) in this zone also demonstrates a clear decreasing tendency with increased $|AL|$. It is known that diffuse auroral lumi-

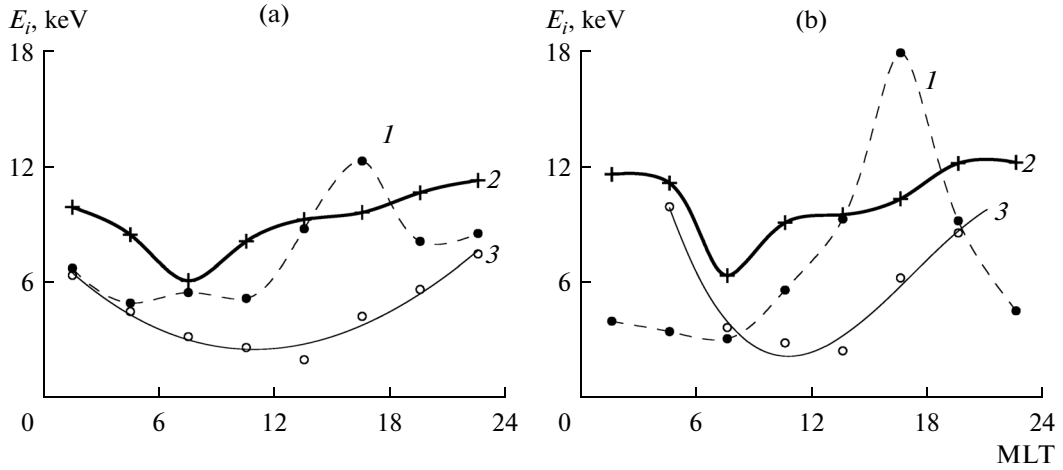

Fig. 2. Diurnal ion energy variations in the DAZ, AOP, and SDP precipitation zones at different magnetic activities. Notes are the same as Fig. 1. (a) $AL = -200$ nT; (b) $AL = -1000$ nT.

nosity equatorward of the auroral oval becomes brighter and more clearly expressed during magnetic disturbances. This indicates that the main source of diffuse luminosity in the midnight sector is the precipitating electrons with an energy flux that increases with an increase in $|AL|$ but not precipitating ions.

Studies analogous to the one shown in Fig. 1 were carried out in all 3-hours MLT sectors, and this allowed us to consider the ion characteristics on a planetary scale. Diurnal variations in the average ion energy (E_i) in different precipitation zones are presented in Fig. 2. The horizontal axis corresponds to the magnetic local time (MLT). The designation of the precipitation zones is the same as in Fig. 1. Approximation of the experimental points in Fig. 2 was made automatically by spline method in the Grapher software (Windows OS). Figures 2a and 2b correspond to low and high levels of magnetic activity ($AL = -20$ and -1000 nT), respectively.

As is seen in Fig. 2, ion energies clearly peak in the postmidday sector 1500–1800 MLT in DAZ (curves *1*). The average energy in the peak increases as magnetic activity increases and is about 12 and 18 keV at $AL = -200$ and -1000 nT, respectively. In the AOP zone (curves *2*), the minimal average ion energies are observed in the sector of 0600–0900 MLT. The energy value in the minimum weakly depends on the magnetic activity level. Detailed ion characteristics in the sectors of 1500–1800 and 0600–0900 MLT are presented in (Vorobjev and Yagodkina, 2014). In the SDP zone (curves *3*), the average ion energies are minimal in the midday sector and gently increase throughout the dawn and dusk sectors, peaking in the midnight sector. No considerable changes in ion energy with an increase in magnetic activity were discovered in the midday sector, while the ion energy slightly increased with increased $|AL|$ in the night-time sectors.

The diurnal distribution of energy flux of precipitating ions is shown in the top panel of Fig. 3 for low (a) and high (b) magnetic activity levels. Notations for the precipitation zones and values of the *AL* index are the same as Fig. 2. In DAZ (curves *1*), the clear peak of precipitation flux is observed in the postmidday sector. The energy flux value nearly doubles with an increase in $|AL|$ from 200 to 1000 nT, while F_i changes insignificantly in the other MLT sectors. In terms of shape, curves *1* in Fig. 3 are generally the same as the curves 1 for diurnal distribution of average ion energies in Fig. 2.

In the AOP zone, ion energy flux is maximal in the nightside MLT sectors. Comparing the curves *2* in Figs. 3a and 3b, we note that an increase in magnetic activity is accompanied by an increase in F_i exclusively in the nightside sectors from 1800 to 0600 MLT. In the daytime and postmidday periods (0900–1800 MLT), ion energy flux weakly changes, even upon such an abrupt increase in *AL* from 200 to 1000 nT. In the SDP zone (curves *3*), the opposite situation is observed: the maximal ion energy flux is observed in the daytime sectors, while F_i values are insignificant in the nighttime ones. Ion energy flux in the *SDP* zone shows a negative correlation with their average energies. In the midday sector, ion energy flux is maximal, but average energies are minimal. This is most clearly seen from a comparison of the curves *3* in Figs 2b and 3b.

The bottom panel of Fig. 3 illustrates the diurnal variation in the values of the F_i/F_e ratio of ion to electron energy flux. It is seen from figures that electron energy flux dominates in most precipitation zones, excluding the postmidday sector of DAZ, where $F_i \approx F_e$ at low magnetic activity (Fig. 3a) and F_i exceeds F_e by the factor of more than 3 at high magnetic activity (Fig. 3b). The detailed comparison between characteristics of ion and electron precipitations in the post-

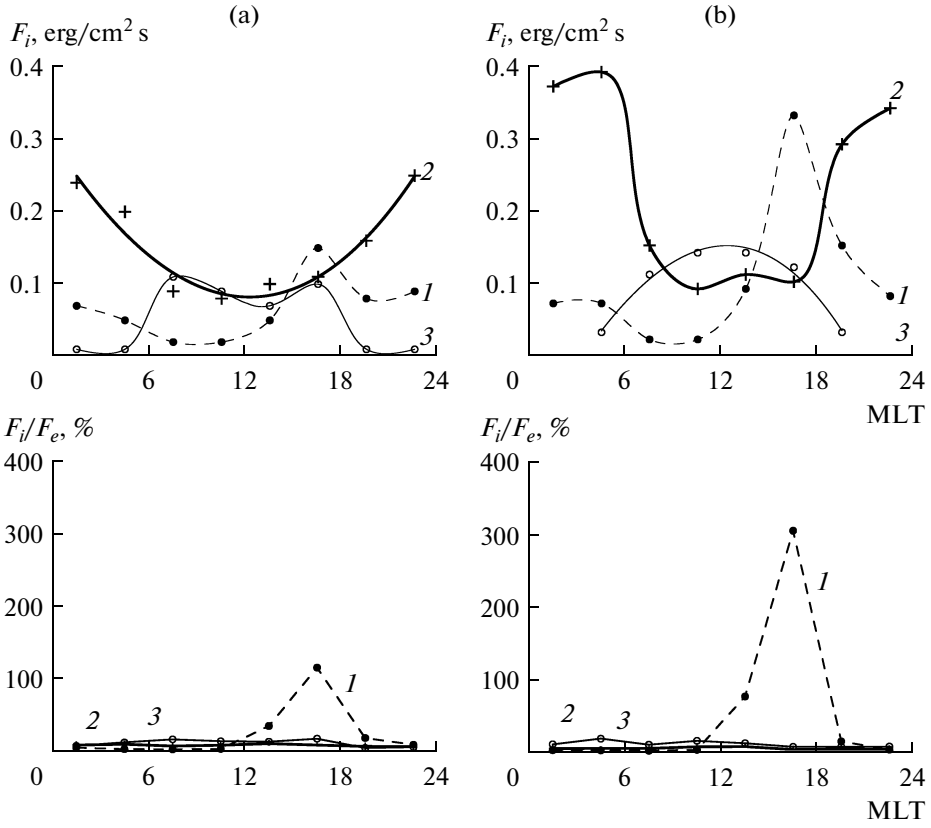

Fig. 3. Diurnal distribution of ion energy flux (top panel) and the value of the ratio between ion and electron energy fluxes (bottom panel) at low (a) and high (b) magnetic activity. Magnetic activity levels and designations of the precipitation zones are the same as Fig. 2.

midday sector is presented in (Vorobjev and Yagodkina, 2014).

The data obtained in our study allowed us to construct a planetary distribution pattern for both average energies and precipitating ion energy fluxes. These distributions can be calculated for all magnetic activity levels expressed by *AL* and *Dst* indices. To recall, the *Dst* index does not determine the characteristics of precipitating particles but considerably affects the positions of precipitation boundaries. The top panel of Fig. 4 illustrates the planetary distribution of ion energy fluxes at low (a) and high (b) magnetic activity. The values of energy flux are given in grayscale (see right part of the figure). Analogous to the APM model, the AOP zone in the nightside is divided by the *b4s* boundary into the equatorial and polar parts (Vorobjev et al., 2013a).

The bottom panel of Fig. 4 illustrates the planetary distribution of F_i/F_e ratio. The values of F_i/F_e are given in grayscale. It is seen that ions of auroral energies play a significant role only in the equatorial part of precipitations, in the afternoon, where the value of F_i/F_e ratio reaches 3 in the sector of 1500–1800 MLT.

The ion precipitation model allowed us to calculate the total energy release (W_i) by ion precipitation on the scale of the entire hemisphere. The value of W_i is not given in the present article; however, Fig. 5 exhibits the most interesting, in our opinion, value of the W_i/W_e ratio depending on the magnetic activity level. Here, W_e is the planetary power of electron precipitation, the numerical values of which were computed from the APM. It is seen in Fig. 5 that the ion contribution to the total energy release is maximal at low magnetic activity and rapidly decreases with increased $|AL|$. The value of the W_i/W_e ratio is about 11% under quiet conditions and decreases to about 4% at $|AL| =$ 1000 nT. It was already noted earlier that the ion precipitation contribution to the total energy release tends to decrease with increasing magnetic activity (Coumans et al., 2004): these authors reported that the proton contribution to the total ionospheric conductance was higher in the quiet periods compared to the substorms.

In (Vorobjev et al., 2013a), the relative error of defining electron precipitation power was estimated at 20–25%. The total contribution of ion precipitation was 10–12% at maximum, and this was nearly twice as low as the relative error of defining electron precipitation power. Thus, the ion precipitation contribution to some processes within the high-latitude ionosphere

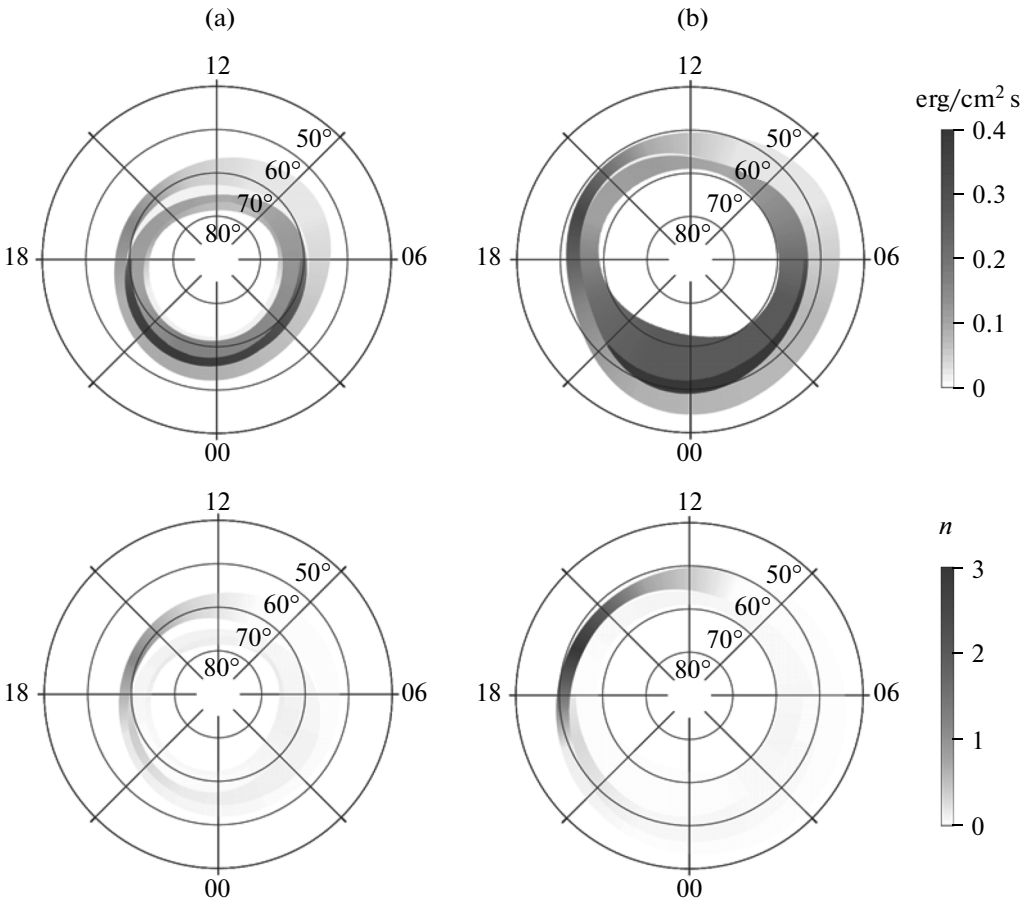

Fig. 4. Planetary distribution of ion fluxes (top panel) and ratio between ion and electron energy fluxes (bottom panel). (a) $AL = -200$ nT and $Dst = -5$ nT; (b) $AL = -1000$ nT and $Dst = -50$ nT.

can be disregarded (for example, when computing the luminosity of main auroral emissions of 427.8, 557.7, and 630.0 nm). This is applicable to all MLT sectors, excluding the postmidday one, in which ion flux may be significant in the equatorial part of auroral precipitations.

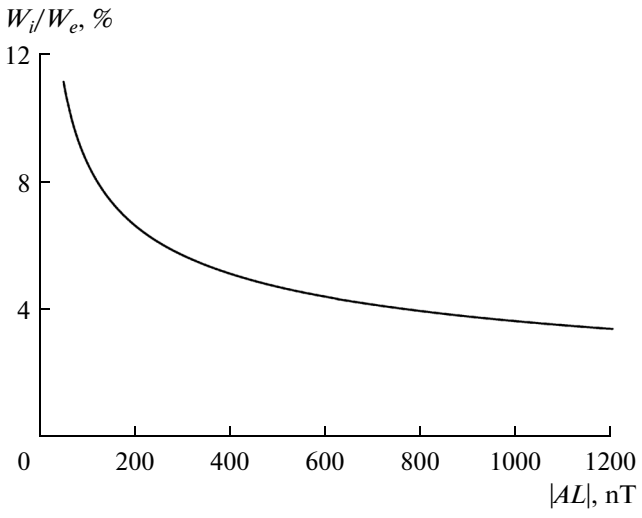

Fig. 5. W_i/W_e ratio between planetary power of ion and electron precipitations depending on magnetic activity.

4. PLASMA PRESSURE AND IONOSPHERIC CONDUCTANCE

4.1. Plasma Pressure

In this section, we will consider some aspects of how to apply the ion precipitation model for different geophysical purposes. Due to the specificity of the formation of an excited hydrogen atom, ion (proton) precipitations dominate in exciting of hydrogen emissions. The ion temperature in the high-latitude magnetosphere several times exceeds that of electrons; therefore, the plasma pressure at the ionosphere altitude is determined chiefly by ion precipitation flux in zones in which the field-aligned potential drop much lower than ion temperature. Ion flux also makes the certain contribution into making up the ionospheric conductance, especially in the postmidday and dusk sectors. Discussion of exciting of the hydrogen emissions was beyond the scope of the present paper; we

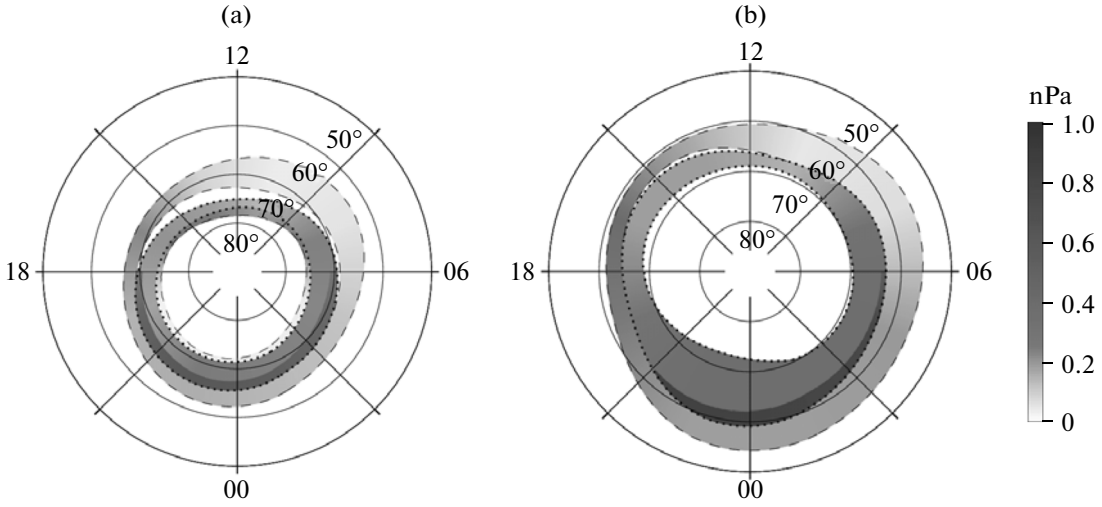

Fig. 6. Planetary distribution of ion pressure at low (a) and high (b) magnetic activity: (a) $AL = -200$ nT and $Dst = -5$ nT; (b) $AL = -1000$ nT and $Dst = -50$ nT. Dotted lines denote the boundaries of the AOP zone; dashed lines show the boundaries of the DAZ and SDP zone.

will only consider in brief some aspects related to plasma pressure and ionospheric conductance.

The method for determining plasma pressure from DMSP satellite measurements was discussed in (Wing and Newell, 1998). In the present article, we will use a modified version of this method for the same purpose (Stepanova et al., 2002, 2006). The computation results are shown in Fig. 6: the planetary distribution of ion pressure at low (a) and high (b) magnetic activity. Plasma pressure was defined within the boundaries of electron precipitation of different types. The AOP boundaries in Fig. 6 are marked with a dotted line. The DAZ (equatorward precipitation) and SDP (poleward precipitation) boundaries are marked with a dashed line. The plasma pressure values in different zones are given in grayscale (the right side of the figure).

In (Antonova et al., 2014), the data shown in Fig. 6a have already been used for comparative analysis of plasma pressure distribution in the ionosphere and the equatorial plane of the magnetosphere. In general, data from low-orbit satellites were used in earlier publications (Wing and Newell, 1998; Stepanova et al., 2006; Wing et al., 2007) to analyze the plasma characteristics in the plasma sheet of the magnetosphere. These studies are based on the following concepts. In the isotropic plasma region, such plasma parameters as pressure, temperature, and density are constant along the same geomagnetic field lines (Goertz and Baumjohann, 1991). Thus, the characteristics of magnetospheric plasma can be obtained by projecting ionospheric data to the equatorial plane of the magnetosphere with the use of some of magnetic field model (MFM). Wing and Newell (1998) characterize all precipitations at the ionosphere altitudes between the *b2i* and *b5* boundaries (Newell et al., 1996) as isotropic ones. In fact, this zone between the *b2i* and *b5* boundaries coincides with the nightside part of the AOP zone, according to the terms used in the present work. The key element in the studies mentioned above is the magnetic field model (MFM). The obtained finally spatial distribution of plasma characteristics in the equatorial plane specifically depends on the accuracy of such model under the conditions of different geomagnetic activity.

In (Antonova et al., 2014), another approach was used: it excluded the MFM influence on the results. In this article, the obtained pressure distribution (Fig. 6a) was compared to the mean statistical distribution of plasma pressure in the equatorial plane of the magnetosphere based on direct measurements by THEMIS satellites (Kirpichev and Antonova, 2011). It was shown in (Antonova et al., 2014) that the source of AOP's nightside part is plasma located in the magnetosphere tail at the geocentric distances from ~6 to ~10–12 Re. In this part of the magnetospheric plasma sheet, the plasma pressure was nearly isotropic (Antonova et al., 2014).

It should be noted that pressure values in Fig. 6 are smaller than the plasma pressure in the equatorial plane. This has several causes. First, the contribution of electrons to the total plasma pressure (this contribution can make up to 15% (Baumjohannet al., 1989)) has not been taken into account. Second, the possible existence of a field-aligned potential drop has also not been taken into consideration (the potential difference can accelerate electron flux but decelerates ions); Antonova et al. (2014), however, attempted to minimize this factor by choosing magnetically quiet intervals for their study. Third, the method of pressure calculation (Stepanova et al., 2002, 2006) implies both an isotropic distribution of particles on pitch angles and Maxwell distribution on energies. However, in con-

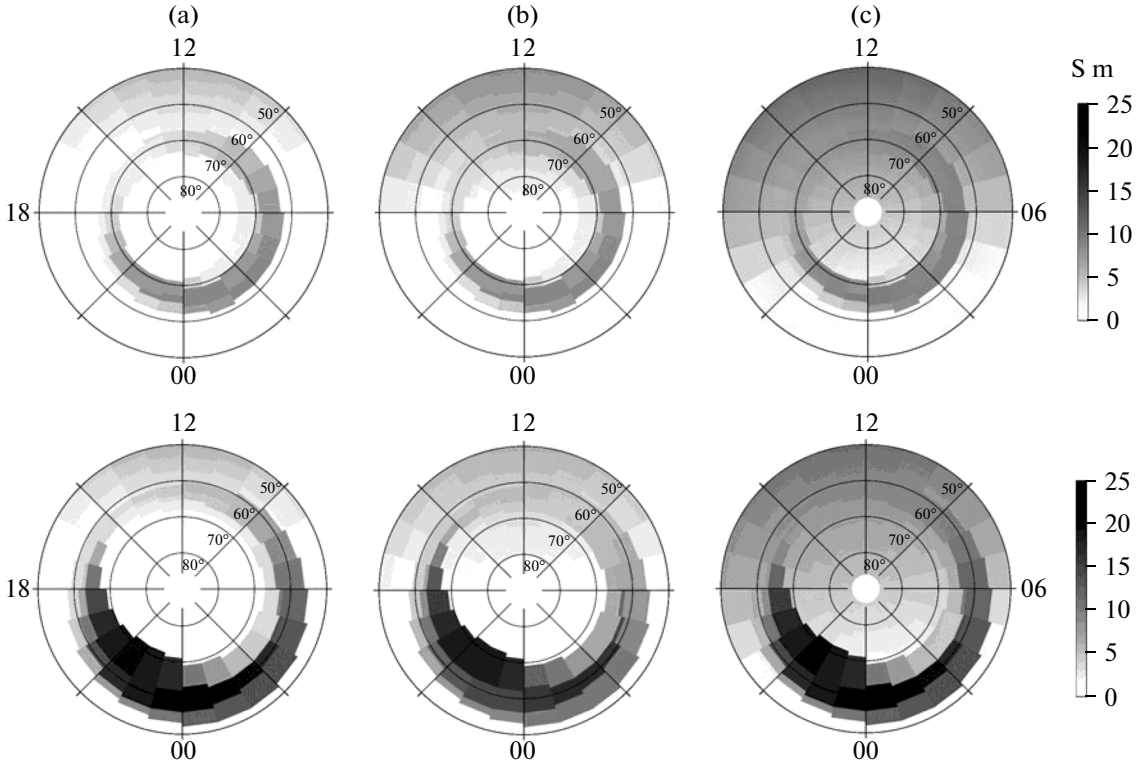

Fig. 7. Planetary distribution of Hall conductance at 1200 UT produced by ion and electron energy fluxes. Top panel: $AL = -200$ nTl and $Dst = -5$ nT. Bottom panel: $AL = -1000$ nT and $Dst = -50$ nT. (a) winter, (b) equinox, (c) summer.

trast to electrons, ions are better described by kappa-distribution (Christon et al., 1991), i.e., the distribution function has a Maxwellian tail in the high-energy part of the spectrum, and this tail can make certain contribution into pressure. The estimates by Antonova et al. (2014) suggest that this error can reach ~20% at the AOP latitudes. Finally, in addition to protons, precipitating particle fluxes contain other components, for example, helium and oxygen ions. Since the contributions of these components cannot be distinguished from the total ion flux by data from DMSP satellites, underestimation of the pressure can reach 15–18% (Kistler et al., 1993). In general, although the ion pressure calculated from DMSP data is lower than the plasma pressure in the equatorial plane, it is still sufficiently high, especially in the equatorial part of AOP (~1 nPa). These values considerably exceed the plasma pressure within the plasma layer, which is a zone with magnetic field lines extremely elongated to the tail. It should be noted that the typical values of plasma pressure on the geostationary orbit are close to 1 nPa (Riazantseva et al., 2000).

4.2. Ionospheric Conductance

The APM model from (Vorobjev et al., 2013a) and the ion precipitation model from the present work were used to simulate the planetary distribution of integral ionospheric conductance. As an example, Fig. 7 shows the model distributions of Hall conductance for the quiet (top) and disturbed (bottom) conditions. The presence of conductance models is essential for studying the electrodynamics of high-latitude ionosphere. Jointly with the data of magnetometric observations, these models make it possible to obtain the global distribution pattern of electrical fields and field-aligned currents and to estimate Joule heating of the ionosphere. Various computational techniques and simulation results for ionospheric conductance are discussed in many publications, for example, in (Robinson et al., 1987; Brekke and Moen, 1993; Galand and Richmond, 2001; Coumans et al., 2004; Nikolaeva et al., 2014).

Figure 7 presents the distributions of total Hall conductance produced by both electron and ion precipitations. Total conductance was calculated as the square root of the sum of squared conductances produced by electrons and ions (Galand et al., 2001). The conductance values (in siemenses) are given in gray-scale (see the right part of the figure). The latitudes in figure are shown with 10° steps beginning from 50°.

Our goal was not to perform an accurate calculation of conductance but rather to show the possible application of the electron and ion precipitation models developed in the framework of our studies for this purpose. Hence, both the Hall and Pedersen conductances were calculated with analytical expressions

from (Robinson et al., 1987; Galand and Richmond, 2001). In these publications, conductances separately caused by electron and ion precipitations were defined as functions of average energies (E_e, E_i) and energy fluxes (F_e, F_i) of precipitating particles. Numerical values of E_e, E_i, F_e, and F_i can be easily found from the precipitation models presented above. In (Robinson et al., 1987; Galand and Richmond, 2001), ionospheric conductance was calculated under the assumption of a Maxwell distribution of energies for both electron and ion precipitations. The composition of neutral atmosphere was taken from the MSIS-90 model for the latitude of auroral zone.

In addition to the precipitating particles, a considerable contribution to ionospheric conductance is made by solar UV and X-ray radiation. The planetary distribution of this conductance (let us name it background conductance hereinafter) depends on both season and universal time. The distribution of background conductance shown in Fig. 7 is presented after the computations on the basis of the GSM TIP model (Namgaladze et al., 1990, 1991) for winter season (a), equinox (b), and summer season (c) at 1200 UT. For the convenience of the possible use of global conductance distribution in practice, the conductance model is subdivided into cells of 1° on latitude and 15° on longitude. The data on the average energies and energy fluxes of precipitating particles in each cell were obtained by approximation of the initial data by a spline function analogous to that in Figs. 2 and 3.

CONCLUSIONS

The data from DMSP *F*6 and *F*7 satellites for 1986 were used to investigate the planetary distribution of ion precipitations. The ion characteristics were defined within three main auroral precipitation zones (after (Starkov et al., 2002)): auroral oval precipitation (AOP), diffuse auroral zone (DAZ), and soft diffuse precipitation (SDP), with the last two zones being located equatorward and poleward of the AOP, respectively.

The influence of magnetic activity on the characteristics of precipitating ions in the sector 2100–2400 MLT has been studied in detail. The choice of this longitudinal interval is based on the fact that the main processes related to development of substorms occur there. The research has shown that in the average energies of precipitating ions in the AOP zone do not depend on the *AL* index. However, ion energy fluxes in the same zone increase with increased magnetic activity: at a constant energy of precipitating ions, such a situation corresponds to an increase in ion concentration. In DAZ, considerable softening of the precipitating ion is observed in the premidnight hours with increased magnetic activity. The average ion energies decrease from 8–10 keV under quiet conditions to 3–5 keV at $|AL| \sim 1000$ nT. Ion energy fluxes in this zone also show a clear decreasing tendency with increased $|AL|$.

On the basis of studying the planetary distribution of ion precipitation characteristics, we made the following conclusions.

(1) For both ion and electron precipitations, no dependence of average energy and energy flux on the *Dst* index has been revealed. In other words, in all precipitation zones and in all MLT sectors, the characteristics of precipitating particles do not depend on the intensity of magnetic storms.

(2) In DAZ, precipitating ion energies have a clear peak in the postmidday sector 1500–1800 MLT. The average energy value in this peak grows as magnetic intensity increases and is ~12 keV at at $AL = -200$ nT and ~18 keV at $AL = -1000$ nT. The energy flux in the peak increases nearly by a factor of 2 as $|AL|$ increases from 200 to 1000 nT, while the energy flux in the remaining MLT sectors changes insignificantly with increased magnetic activity.

(3) In the AOP zone, the minimal average ion energy is observed in the dawn sector 0600–0900 MLT. The energy value in the minimum weakly depends on magnetic activity. Ion energy fluxes (F_i) are maximal in the nightside MLT sectors. An increase in magnetic activity is accompanied by an increase in F_i only in the hight-time hours, while F_i weakly changes in the daytime and postmidday hours even with an $|AL|$ increase from 200 to 1000 nT.

(4) In the SDP zone, the highest ion energy fluxes are observed in the daytime sector, while F_i in the nightside sectors is insignificant. Ion energy fluxes in the SDP zone show an anticorrelation to average ion energies. In the midday sector, ion energy fluxes are maximal, but ion average energies are minimal, and vice versa in the midnight sector.

(5) On the basis of the direct measurements obtained by DMSP satellites, an ion precipitation model has been developed. This model allows us to obtain the planetary distribution of average ion energies and ion energy fluxes depending on magnetic activity level expressed by values of the *AL* and *Dst* indices. Comparison of the ion and electron precipitation models shows that the planetary power of ion precipitations at low magnetic activity ($|AL| = 100$ nT) is ~12% of the electron precipitation power and exponentially decreases to ~4% at $|AL| > 1000$ nT.

The ion precipitation model allows the plasma pressure at the ionosphere altitudes to be calculated at different geomagnetic activities. The planetary ion pressure distribution in the magnetic quiet period was used in (Antonova et al., 2014) for comparative analysis of plasma pressure distribution in the ionosphere and in the equatorial plane of the magnetosphere. It was shown that plasma pressure in the equatorial AOP zone is close to the value of plasma pressure near geostationary orbit.

The ion and electron precipitation models were used to calculate the planetary distribution of integral Hall and Pedersen ionospheric conductances depending on the magnetic activity (*AL* and *Dst* indices), season (winter, summer, equinox), and universal time (UT).

ACKNOWLEDGMENTS

The work was supported by the Presidium of the Russian Academy of Sciences (program no. 9). E.E. Antonova was supported in part by the Russian Foundation for Basic Research (project no. 15-05-04965).

We thank V.V. and M.V. Klimenko for the data on background ionospheric conductance. The measurements of DMSP *F*6 and *F*7 satellites were taken from http://sd-www.jhuapl.edu; the values of magnetic activity indices are from http://wdc.kugi.kyoto-u.ac.jp/dst_final/198602/index.html.

REFERENCES

Antonova, E.E., Kirpichev, I.P., and Stepanova, M.V., Plasma pressure distribution in the surrounding the Earth's plasma ring and its role in the magnetospheric dynamics, *J. Atmos. Sol.-Terr. Phys.*, 2014, vol. 115, pp. 32–40. doi: 10.1016/j.jstp.2013.05.007

Antonova, E.E., Ermakova, N.O., Stepanova, M.V., and Teltsov, M.V., The influence of the energetic tails of ion distribution function on the main parameter of the theory of field-aligned current splitting and Intercosmos-Bulgaria-1300 observations, *Adv. Space Res.*, 2003, vol. 31, no. 5, pp. 1229–1234.

Antonova, E.E., Vorob'ev, V.G., Kirpichev, I.P., and Yagodkina, O.I., Comparison of the plasma pressure distributions over the equatorial plane and at low altitudes under magnetically quiet conditions, *Geomagn. Aeron.*, 2014, vol. 54, no. 3, pp. 278–281.

Baumjohann, W., Paschmann, G., and Cattell, C.A., Average plasma properties in the center plasma sheet, *J. Geophys. Res.*, 1989, vol. 94, no. 6, pp. 6597–6606.

Brekke, A. and Moen, J., Observations of high-latitude ionospheric conductances, *J. Atmos. Terr. Phys.*, 1993, vol. 55, nos. 11–12, pp. 1493–1512.

Coumans, V., Gerard, J.-C., and Hubert, B., Electron and proton excitation of the FUV aurora: Simultaneous IMAGE and NOAA observations, *J. Geophys. Res.,* vol. 107, no. A11, p. 1347. doi: 10.1029/2001JA009233

Coumans, V., Gerard, J.-C., Hubert, B., Meurant, M., and Mende, S.B., Global auroral conductance distribution due to electron and proton precipitation from image-FUV observations, *Ann. Geophys.*, 2004, vol. 22, pp. 1595–1611.

Criston, S.P., Williams, D.J., Mitchell, D.J., Huang, C.Y., and Frank, L.A., Spectral characteristics of plasma sheet ion and electron populations during disturbed geomagnetic conditions, *J. Geophys. Res.*, 1991, vol. 96, no. 1, pp. 1–22.

Galand, M. and Richmond, A.D., Ionospheric electrical conductances produced by auroral proton precipitation, *J. Geophys. Res.*, 2001, vol. 106, no. A1, pp. 117–125.

Galand, M., Fuller-Rowell, T.J., and Codrescu, M.V., Response of the upper atmosphere to auroral protons, *J. Geophys. Res.*, 2001, vol. 106, no. A1, pp. 127–139.

Goertz, C.K. and Baumjohann, W., On the thermodynamics of the plasma sheet, *J. Geophys. Res.*, vol. 96, no. A12, pp. 20991–20998. doi: 10.1029/91JA02128

Hardy, D.A., Gussenhoven, M.S., and Brautigan, D., A statistic model of auroral ion precipitation, *J. Geophys. Res.*, 1989, vol. 94, no. A1, pp. 370–392.

Kirpichev, I.P. and Antonova, E.E., Plasma pressure distribution in the equatorial plane of the Earth's magnetosphere at geocentric distances of 6–10 R_E according to the international THEMIS mission data, *Geomagn. Aeron.*, 2011, vol. 51, no. 4, pp. 450–455.

Kistler, L.M., Baumjohann, W., Nagai, T., and Mobius, E., Superposed epoch analysis of pressure and magnetic field configuration changes in the plasma sheet, *J. Geophys. Res.,* 1993, vol. 98, no. A6, pp. 9249–9258.

Liou, K., Newell, P.T., Sibeck, D.G., Meng, C.-I., Brittnacher, M., and Parks, G., Observations of IMF and seasonal effects in the location of auroral substorm onset, *J. Geophys. Res.*, 2001, vol. 106, no. A4, pp. 5799–5810.

Maltsev, Yu.P., Points of controversy in magnetic storm studying, *Space Sci. Rev.*, 2004, vol. 110, pp. 227–277.

Namgaladze, A.A., Korenkov, Y.N., Klimenko, V.V., Karpov, I.V., Suronkin, V.A., and Naumova, N.M., Numerical modeling of the thermosphere–ionosphere–protonoshpere system, *J. Atmos. Terr. Phys.*, 1991, vol. 53, pp. 1113–1124.

Namgaladze, A.A., Koren'kov, Yu.N., Klimenko, V.V., Karpov, I.V., Bessarab, F.S., Surotkin, V.A., Glushchenko, T.A., and Naumova, N.M., Global numerical model of the thermosphere, ionosphere, and protonosphere of the Earth, *Geomagn. Aeron.*, 1990, vol. 30, no. 4, pp. 612–619.

Newell, P.T., Sotirelis, T., and Wing, S., Diffuse, monoenergetic and broadband aurora: The global precipitation budget, *J. Geophys. Res.*, 2009, vol. 114, no. A9, p. A09207. doi: 10.1029/2009JA014326

Newell, P.T., Rouhoniemi, J.M., and Meng, C.-I., Maps of precipitation by source region, binned by IMF, with inertial convection streamlines, *J. Geophys. Res.*, vol. 109, p. A10206. doi: 10.1029/2009JA010499

Newell, P.T., Feldstein, Ya.I., Galperin, Yu.I., and Meng, C.-I., Morphology of nighttime precipitation, *J. Geophys. Res.*, 1996, vol. 101, no. A5, pp. 10737–10748. doi:

Nikolaeva, V.D., Kotikov, A.L., and Sergienko, T.I., Dynamics of field-aligned currents reconstructed by the ground-based and satellite data, *Geomagn. Aeron.*, 2014, vol. 54, no. 5, pp. 549–557.

Riazantseva, M.O., Sosnovets, E.N., Teltsov, M.V., and Vlasova, N.A., Geostationary orbit plasma pressure variations according to Gorizont satellite data, *Adv. Space Res.*, 2000, vol. 25, no, 12, pp. 2365–2368. doi: 10.1016/S0273-1177(99)00524-4

Robinson, R.M., Vondrak, R.R., Miller, K., Dabbs, K., and Hardy, D., On calculating ionospheric conductances from the flux and energy of precipitating electrons, *J. Geophys. Res.*, 1987, vol. 92, no. 3, pp. 2565–2569.

Starkov, G.V., Rezhenov, B.V., Vorob'ev, V.G., Fel'dshtein, Ya.I., and Gromova, L.I., Dayside auroral precipitation structure, *Geomagn. Aeron.*, 2002, vol. 42, no. 2, pp. 176–183.

Stepanova, M.V., Antonova, E.E., Bosqued, J.M., Kovrazhkin, R.A., and Aubel, K.R., Asymmetry of auroral electron precipitations and its relationship to the substorm expansion phase onset, *J. Geophys. Res.,* 2002, vol. 107, no. A7. doi: 10.1029/2001JA003503

Stepanova, M., Antonova, E.E., and Bosqued, J.-M., Study of plasma pressure distribution in the inner magnetosphere using low-altitude satellites and its importance for the large-scale magnetospheric dynamics, *Adv. Space Res.*, 2006, vol. 38, pp. 1631–1636.

Vorob'ev, V.G., Gromova, L.I., Rezhenov, B.V., Starkov, G.V., and Feldshtein, Ya.I., Variations of the boundaries of plasma precipitations and auroral luminosity in the nighttime sector, *Geomagn. Aeron.*, 2000, vol. 40, no. 3, pp. 344–350.

Vorobjev, V.G., Yagodkina, O.I., and Katkalov, Y., Auroral precipitation model and its applications to ionospheric and magnetospheric studies, *J. Atmos. Sol.-Terr. Phys.*, 2013a, vol. 102, pp. 157–171. doi: 10.1016/j.jstp.2013.05.007

Vorobjev, V.G., Kirillov, A.S., Katkalov, Yu.V., and Yagodkina, O.I., Planetary distribution of the intensity of auroral luminosity obtained using a model of aurora precipitation, *Geomagn. Aeron.*, 2013b, vol. 53, no. 6, pp. 711–715.

Vorobjev, V.G. and Yagodkina, O.I., Comparative characteristics of ion and electron precipitation in the dawn and dusk sectors, *Geomagn. Aeron.*, 2014, vol. 54, no. 1, pp. 50–58.

Wing, S. and Newell, P.T., Center plasma sheet ion properties as inferred from ionospheric observations, *J. Geophys. Res.,* 1998, vol. 103, no. A4, pp. 6785–6800.

Wing, S., Gjerloev, J., Johnson, J.R., and Hoffman, R.A., Substorm plasma sheet ion pressure profile, *Geophys. Res. Lett.*, 2007, vol. 34, p. L16110. doi: 10.1029/2007GL030453

Translated by N. Astafiev